Regulation of Colorectal Cancer Cell Apoptosis by the n-3 Polyunsaturated Fatty Acids Docosahexaenoic and Eicosapentaenoic

Anna Giros,[1] Mike Grzybowski,[1] Vanessa R. Sohn,[1] Elisenda Pons,[2] Jessica Fernandez-Morales,[2] Rosa M. Xicola,[1] Puja Sethi,[1] Jessica Grzybowski,[1] Ajay Goel,[3] C. Richard Boland,[3] Miquel A. Gassull[2] and Xavier Llor[1]

Abstract Several studies have suggested that the n-3 fatty acids Docosahexaenoic (DHA) and Eicosapentaenoic (EPA) have an important protective effect on colorectal cancer, and this could be at least partly due to their proapoptotic activity. It is unclear, however, how this phenomenon is triggered and what mechanisms are implicated. Here, we show that both DHA and EPA have an important proapoptotic effect on colorectal cancer cells with different molecular phenotypes but not in noncancerous cells. Apoptosis is caspase dependent, and both intrinsic and extrinsic pathways are implicated. The dimerization of Bax and Bak, the depolarization of the mitochondrial membrane, and the subsequent release of cytochrome *c* and Smac/Diablo to the cytosol evidence the activation of the intrinsic pathway. The implication of the extrinsic pathway is shown by the activation of caspase-8, along with the down-regulation of *FLIP*. The timing of caspase-8 activation, and the oligomerization of Bid with Bax, suggest a cross-talk with the intrinsic pathway. None of the death receptors that commonly initiate the extrinsic pathway: FAS, TNF-R1, and TRAIL-R2 are found to be responsible for triggering the apoptosis cascade induced by DHA and EPA. Neither PPARγ nor cyclooxygenase-2, two likely candidates to regulate this process, play a significant role. Our findings suggest that the down-regulation of two key regulatory elements of the extrinsic and intrinsic pathways, FLIP and XIAP, respectively, is determinant in the induction of apoptosis by DHA and EPA. These fatty acids could potentially be useful adjuvant anticancer agents in combination with other chemotherapeutic elements.

Colorectal cancer is the second leading cause of cancer-related death in developed countries (1). Environmental (mostly dietary) and lifestyle factors can be accounted for the large differences in the incidence observed around the world (2). Several epidemiologic and case-control studies have suggested a decrease in colorectal cancer risk among individuals consuming diets high in n-3 polyunsaturated fatty acids (PUFA; refs. 3–6). Docosahexaenoic (DHA) and eicosapentaenoic (EPA) are important long-chain polyunsaturated ω-3 fatty acids, which are abundant in fish oil. Mammals are unable to synthesize neither n-3 nor n-6 PUFAs and they have to obtain them from the diet. Both n-3 and n-6 PUFAs are important constituents of cell membranes. Cell membrane fatty acid composition of both normal and neoplastic tissues undergo modification in animals fed different fat diets, reflecting the fatty acid content of the consumed lipid (7). This may affect many membrane properties, such as permeability or lipid packing, gene expression, transcription factor activity, signal transduction, or the activity of specific proteins, such as protein kinase C or ornithine decarboxylase (8–10). Some of these changes could ultimately drive the antineoplastic effect of n-3 PUFAs. Cyclooxygenase (Cox)-2 inhibition has also been suggested to mediate the anticarcinogenic effects of DHA and EPA on colorectal cancer (9). N-3 PUFAs compete with n-6 PUFAs for desaturases that metabolize them to longer chain fatty acids. Increasing the dietary intake of n-3 PUFAs decreases the desaturation of the n-6 PUFA linoleic acid and its subsequent formation of arachidonic acid (11). Arachidonic acid is the substrate for prostaglandin production through Cox activity. Prostaglandins and Cox-2 may facilitate colon cancer progression by stimulating cell proliferation and survival, tumor cell invasiveness, and the production of angiogenic agents (12).

Apoptosis, or programmed cell death, is an essential component of cell number regulation in colonic epithelia and a crucial mechanism to prevent damaged or mutated cells from surviving and dividing, hence contributing to carcinogenesis. The capacity of n-3 PUFAs to induce colonocyte apoptosis has been

Authors' Affiliations: [1]Department of Medicine and Cancer Center, University of Illinois at Chicago, Chicago, Illinois; [2]Fundació Institut d'Investigació en Ciències de la Salut Germans Trias i Pujol. Catalonia, Spain; and [3]Department of Medicine and Cancer Center. Baylor University Medical Center. Dallas, Texas
Received 10/23/08; revised 5/3/09; accepted 5/14/09; published OnlineFirst 7/28/09.

Grant support: Internal Grant from Department of Medicine and Cancer Center. University of Illinois at Chicago, and Grant N: PI050850 from Fondo de Investigacion Sanitaria. Spain's Ministerio de Sanidad y Consumo.

Note: Supplementary data for this article are available at Cancer Prevention Research Online (http://cancerprevres.aacrjournals.org/).

Requests for reprints: Xavier Llor, Department of Medicine, University of Illinois at Chicago, 840 South Wood Street (M/C 716), Chicago, IL 60612. Phone: 312-413-8872; Fax: 312-996-5103; E-mail: xllor@uic.edu.

doi:10.1158/1940-6207.CAPR-08-0197

documented in several scenarios. Dietary supplementation with EPA resulted in a significant increase in crypt cell apoptosis in humans with a history of colorectal adenomas (13) as well as in normal rat colonic mucosa (14). This effect has also been seen in rodent models of colorectal carcinogenic induction fed with fish oil as the source of fat (15, 16) as well as in human colorectal adenocarcinoma cells (17, 18).

However, the mechanisms by which these n-3 PUFAs induce apoptosis in colorectal cancer are still largely unknown. Most published studies have only addressed the effects on selected steps or elements implicated in the apoptotic process and often have been limited to single cell models making it difficult to generalize the obtained information.

With the present work, we show that the apoptotic response induced by DHA and EPA in colorectal cancer cells is caspase dependent; there is activation of the extrinsic pathway evidenced by increase of caspase-8 activity along with a reduction of apopotsis upon addition of caspase-8 inhibitor and down-regulation of the crucial inhibitor of this pathway FLIP; there is also a clear activation of the intrinsic pathway, shown by mitochondrial membrane depolarization with subsequent release of cytochrome *c* and Smac/Diablo to the cytosol, caspase-9 activation, dimerization of the Bcl-2 family of proteins Bax and Bak, and down-regulation of the crucial inhibitor of this pathway XIAP. A cross-talk or activation of the intrinsic pathway by the extrinsic pathway is suggested by the oligomerization of Bid with Bax along with a decrease in full length Bid. A suggested apoptosis activation flow graph, according to the described results, is depicted in Fig. 6B.

Materials and Methods

Cell cultures and supplements

To study apoptosis induction, we used five human colon adenocarcinoma cell lines and NCM460, a cell line derived from normal human colon mucosal epithelium. The rest of the experiments were done only with Caco-2 and HT-29 cells. Adenocarcinoma cells were chosen due to their different molecular phenotypes, such as: wild-type p53 (HCT116, LoVo) versus mutated p53 (Caco-2, HT-29, and SW480), microsatellite stable (Caco-2, HT-29, SW480) versus microsatellite unstable (HCT116, LoVo), and wild-type β-catenin (LoVo, SW480, HT-29) versus mutated β-catenin (HCT116, Caco-2). Doubling times in colorectal cancer cells range from 20 h for HCT116 to 62 h for Caco-2, being 32 h for NCM460 cells. Caco-2 and HT-29 cell lines were grown as previously described (17). HCT116, LoVo, and SW480 human colon adenocarcinoma cell lines were grown in 1:1 DMEM with L-glutamine and sodium pyruvate, 100 U/mL penicillin, 100 μg/mL streptomycin, and 10% fetal bovine serum. NCM460 was grown in INCELL's enriched M3:10ä medium (M3 medium plus supplements and 10% fetal bovine serum; INCELL). Cells were maintained at 37°C in a humidified atmosphere containing 5% CO_2. Cell cultures were tested monthly for *Mycoplasma* colonization with VenorGeM Mycoplasma Detection kit reverse transcription-PCR (Sigma-Aldrich).

Cells were plated overnight. The corresponding fatty acid supplements were added daily at a final PUFA nontoxic concentration of 60 μmol/L (see dose-response graphs as Supplementary Fig. S1). Supplements used were EPA and DHA (Cayman Chemical Company) diluted in ethanol. Control conditions consisted of supplementation with ethanol at the same final ethanol concentration present in PUFA-supplemented cells.

Apoptosis assessment by 4′,6-diamidino-2-phenylindole

Morphologic assessment of apoptosis was done with 4′,6-diamidino-2-phenylindole staining and mounted with Vectashield mounting medium as previously described (17). Slides were visualized under a fluorescence microscope and apoptosis was assessed according to morphologic criteria: cell shrinking, membrane blebbing, formation of apoptotic bodies, and chromatin condensation.

Apoptosis quantification by flow cytometry

Cells were trypsinized 24 h postsuplementation, washed with 1×PBS, and stained with annexin V/propidium iodode with Annexin-V-FLUOS (Roche Diagnostics) according to the manufacturer's instructions. Finally, apoptosis was quantified with a FACScan flow cytometer. Apoptosis was also assessed after the addition of several caspase inhibitors: z-VAD-FMK (broad spectrum caspase inhibitor), Ac-DEVD-CHO (caspase-3 specific inhibitor), Ac-IETD-CHO (caspase-8 specific inhibitor), and Ac-LEHD-CHO (caspase-9 specific inhibitor) all from BIOMOL International; as well as Bax Inhibiting Peptide, V5 (Calbiochem); and XIAP recombinant protein (Alexis Biochemicals). All inhibitors were added to a final concentration of 100 μmol/L. The implication of PPARγ in the induction of apoptosis was studied by the addition of the PPARγ ligand troglitazone at 10 μmol/L and an irreversible PPARγ inhibitor, GW9662 at 7.5 μmol/L (Sigma-Aldrich).

Preparation of whole cell protein lysates

Eight million cells were collected by scraping with 1×PBS and lysed with 200 μL of lysis buffer [50 mmol/L Tris (pH 7.5), 150 mmol/L NaCl, 0.5 mmol/L EDTA, and 0.5% Nonidet p-40]. Incubation was carried out with agitation for 40 min at 4°C. Finally, cells were centrifuged at 16,000 *g* for 10 min at 4°C and supernatant was collected. Protein concentration was measured by the Bradford assay (Bio-Rad Laboratories). Experiments were done 2, 4, and 8 h postsupplementation.

Preparation of cytosolic and mitochondrial protein fractions

Twelve million cells were collected by scraping with 1×PBS, resuspended in 500 μL of cold buffer A [50 mmol/L Tris (pH 7.4), 25 mmol/L sucrose, 1 mmol/L EDTA, 1 mmol/L DTT, 0.1 mmol/L phenylmethylsulfonyl fluoride, 1 μg/mL proteases inhibitor cocktail], allowed to swell for 30 min on ice, and finally disrupted by 20 strokes in a Dounce homogenizer. Homogenates were centrifuged at 800 *g* for 10 min at 4°C to pellet nuclei and debris. Supernatants were centrifuged at 14,000 *g* for 40 min at 4°C, and the cytosolic fraction (supernatant) was collected. Pellets were lysed in 100 μL of buffer B [50 mmol/L HEPES (pH 7.4), 1 mmol/L EDTA, 10% glycerol, 1% Triton X-100, 2 mmol/L DTT, 1 μg/mL proteases inhibitors cocktail] for 20 min on ice, and then centrifuged at 14,000 *g* for 40 min at 4°C. The resulting supernatants constituted the mitochondrial fraction. Protein concentration was measured with the Bradford assay. To determine the quality of cytosolic and mitochondrial separation, both fractions were immunoblotted with the mitochondrial marker cytochrome *c* oxidase subunit IV (Molecular Probes). Experiments were done 2, 4, and 8 h postsupplementation.

Caspase activity assay

Caspase activity was measured in whole cell lysates by fluorometric assay using DEVD-AMC, IETD-AMC, and LEHD-AMC (Alexis Biochemicals) as substrates for caspase-3, 8, and 9, respectively. A total of 75 μg of protein lysate were incubated with 10 μmol/L of substrate in assay buffer [50 mmol/L HEPES (pH 7.5), 20% sucrose, 0.2% CHAPS, 10 mmol/L DTT] at 37°C. Caspase substrate cleavage releases 7-amino-4-methoxy coumarin, which emits a fluorescent signal with 380 nm excitation and 460 nm emission. Fluorescence was registered for 3 h at 1-min intervals using a fluorescence reader (Lambda K; Bonsai Technologies). Fluorescence was calibrated using standard curves for AMC concentration. Experiments were done 2, 8, 18, and 24 h postsupplementation.

Determination of mitochondrial membrane depolarization

Cells were stained with the mitochondrial membrane potential marker JC1 (Sigma-Aldrich) for 1 h at 37°C and at a 4 μmol/L concentration. Cells were then rinsed with medium, and afterwards, fresh medium was added to the plates. Mitochondrial membrane potential was determined with fluorescence microscopy. Nondepolarized mitochondria display an orange color and depolarized mitochondria display a green color. Experiments were done 2, 4, 8, 12, and 18 h postsupplementation.

Determination of gene expression

Total RNA was extracted with 1 mL Tripure/10 cm2 (Roche Diagnostics) at different times postsupplementation (from 1 h to 18 h). One microgram of RNA was reverse transcribed to cDNA using a High-Capacity cDNA Archive kit (Applied Biosystems). MicroFluidic cards (Applied Biosystems) were loaded with 50 ng of cDNA plus 50 μL of Taqman gene expression master mix, per well. Four replicates were assayed for each gene: *Bax, Bid, Bcl-2, Bcl-X_L, Cox-2, FLIP, XIAP, Fas, TNF-RI, TRAIL-R2 (DR5)*, and endogenous control (18S ribosomal). Real-time PCR was done with an ABI Prism 7900 (Applied Biosystems). Results were adjusted to endogenous control and normalized to experimental control (ethanol). Ethanol values were taken as the calibrator values, and relative expression (RQ) was calculated with the RQ manager program (Applied Biosystems). RQ values were calculated based on the comparative CT method (19). Graphs reflect the plotted RQ and a RQ of 1 means equal expression as control-supplemented (ethanol) cells. ANOVA was used to assess statistically significant differences. P values of <0.05 were considered statistically significant.

Protein expression analysis

Proteins were separated on a 10% to 12% SDS-polyacrilamide gel and transferred to Immobilon polyvinylidene difluoride membranes (Millipore). Membranes were blocked with 5% nonfat dry milk containing buffer TBS-T [20 mmol/L Tris-HCl (pH 7.5), 150 mmol/L NaCl, 0.1% Tween 20] and incubated for 1 h with the following primary antibodies against XIAP, FLIP, (Cell Signaling Technology), Bax, Bak, Actin, Smac/Diablo (Sigma-Aldrich), and cytochrome *c* (BD Pharmingen). The incubation was overnight with the primary antibodies Bid, Bcl-X_L, TRAIL-R2 (DR5; Cell Signaling Technology), Cox-2 (Cayman Chemical Company), Bcl-2 (Upstate Biotech-Millipore), and TNF-RI, FAS (Santa Cruz Biotechnology, Inc.). Incubation with secondary antibodies was carried out for 1 h with horseradish peroxidase–conjugated goat anti-rabbit or anti-mouse IgG (Cell Signaling Technology). Antibody binding was detected with SuperSignal West Pico (Pierce Biotechnology). Experiments were done 2, 4, and 8 h postsupplementation.

Flow cytometry analysis for TNF-R1 expression

Cells were detached using a cell lifter, and 4×10^6 cells were centrifuged, the pellet washed with cold PBS, and resuspended in 0.5 mL PBS. Then cells were vortexed gently, as 5 mL of 95% ethanol was added to each tube, and stored at 4°C. For staining, 2×10^6 cells were centrifuged, and the pellet resuspended in 2 mL of HCL/Triton (2M HCL, 0.5% Triton X-100), while vortexing gently, and finally incubated at room temperature for 30 min. Then samples were centrifuged and resuspended in 2 mL of borate neutralizing solution and incubated at room temperature for 15 min. Next, the samples were centrifuged, resuspended in 0.4 mL of PBS/Tween/bovine serum albumin (PTB) with 4 μL of primary antibody (TNF-R1 200 μg/mL; Santa Cruz Biotechnology) and incubated for 30 min at room temperature. Then cells were washed twice with cold PTB solution, incubated for an additional 30 min in 150 μL of the PTB with 3 μL of biotinylated secondary antibody (anti-rabbit 1.5 mg/mL; Vector Laboratories). Subsequently, samples were washed twice with PTB and incubated with PTB with fluorescein (FITC) at a 1:100 dilution for 30 min at room temperature. Finally, cells were washed twice with PTB solution, resuspended in 1 mL of 1% para-formaldehyde, and ran through a flow cytometer. All centrifugations were done at 1,000 rpm for 5 min at 4°C. Unlabeled cells and cells labeled with secondary antibody alone served as negative controls. The mean values of fluorescence intensity of 10,000 cells were determined by fluorescence-activated cell sorting (FACS) analysis (BD LSR; BD Biosciences).

Protein coimmunoprecipitation

All coimmunoprecipitations were done with the ProFoundTM Mammalian CoImmunoprecipitation kit (Pierce Biotechnology), and the protocol was carried out according to the manufacturer's instructions. Bax protein from whole cell lysates was precipitated using a specific Bax antibody (Sigma-Aldrich). Samples were ran on a SDS-PAGE gel, transferred to polyvinylidene difluoride membrane, and incubated overnight with the following antibodies: Bax, Bak (Sigma-Aldrich), Bcl-X_L, and Bid (Cell Signaling Technology). Then, samples were incubated for 1 h with horseradish peroxidase–conjugated goat anti-rabbit IgG (Cell Signaling Technology). Finally, antibody binding was detected using SuperSignal West Pico (Pierce Biotechnology).

Statistical analysis

All experiments were repeated at least thrice, and each experiment included at least three replicates per condition. Statistical analysis was done using the Kruskall Wallis one-way ANOVA by rank and the Mann-Whitney U test to assess significant differences in apoptosis. Statistical significance was assumed with a P value of ≤ 0.05.

Results

Apoptosis induction by DHA and EPA

Morphologic changes were evaluated 18 and 24 hours after supplementation with DHA, EPA, or control by 4′,6-diamidino-2-phenylindole staining. At 24 hours, there was already a very significant decrease in the number of cells in the n-3 PUFA–supplemented colorectal cancer wells (Caco-2, HT-29, HCT116, LoVo, SW480) and many of the cells still present displayed clear apoptotic features, such as condensed chromatin, membrane blebbing, and apoptotic bodies. However, there was no evidence of apoptosis induction after supplementation of the normal human colon mucosal epithelium cells NCM460 (Supplementary Fig. S2). Figure 1A shows representative images of Caco-2 and NCM460 cells after DHA and EPA supplementation. Once the proapoptotic effect of DHA and EPA was established in all colorectal cancer cells, we proceeded to quantify apoptosis induction by flow cytometry. There was at least a 10-fold increase in the number of apoptotic cells 24 hours after supplementation with EPA and DHA in relation to control in all cancer cells (Fig. 1B). We then proceeded to study different mechanisms leading to apoptosis at time points between 1 and 24 hours postsupplementation.

Apoptosis induction is caspase-dependent

To show the implication of the different caspase pathways, we quantified caspase activity using a fluorimetric assay. We assessed caspase-3, an executor caspase that is activated by both the intrinsic and the extrinsic pathways; caspase-8, the crucial initiator caspase of the extrinsic pathway, and caspase-9, essential in the activation of the intrinsic pathway. As shown in Fig. 2A, the activity of all three caspases increased as early as 2 hours after n-3 PUFA supplementation. Caspase-3 activity was the highest, which would be expected provided this is an executor caspase for both pathways. The implication of both the intrinsic and extrinsic pathways was further confirmed because there was an increase in both caspase-8 and caspase-9 activities. EPA supplementation resulted in an earlier increase

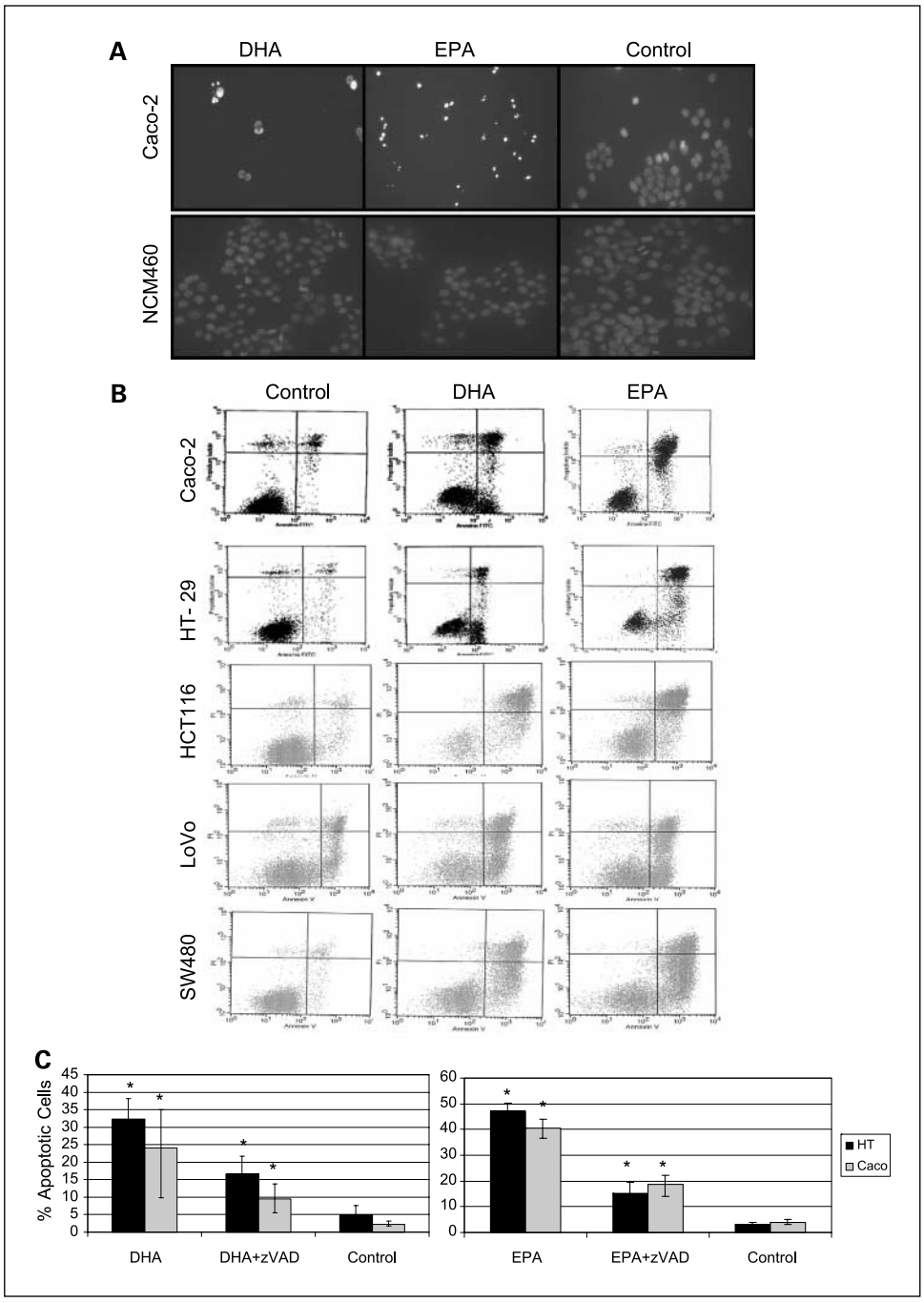

Fig. 1. *A,* fluorescence microscopy images of 4′,6-diamidino-2-phenylindole–stained Caco-2 and NCM460 cells 24 h postsupplement with DHA, EPA, or control. *B,* flow cytometry graphs representing propidium iodide concentration versus Annexin V concentration 24 h postsupplement in Caco-2, HT-29, HCT116, LoVo, and SW480 cells. Left to right, control cells, DHA, and EPA. The apoptotic population (*right bottom quadrant*) and/or late apoptotic population (*right top quadrant*) is always significantly higher in DHA and EPA-supplemented cells. *C,* quantification of apoptotic cells as % over total number of cells 24 h postsupplementation. Black bars, HT-29; gray bars, Caco-2. Left graph, the results for DHA; right graph, the results for EPA. *, statistical significance of $P < 0.05$. Differences are statistically significant in all cases after addition of broad-spectrum caspase inhibitor zVAD.

in caspase activity in HT-29 cells, suggesting a faster effect of EPA on apoptosis induction in these cells.

These results were confirmed with the addition of caspase inhibitors. Thus, the addition of both broad-spectrum caspase inhibitor z-VAD-FMK, and Ac-DEVD-CHO, a caspase-3–specific inhibitor resulted in a dramatic decrease in apoptosis induction, confirming that both DHA and EPA induce apoptosis through caspases (Figs. 1C and 2B). The use of a caspase-8–specific inhibitor (Ac-IETD-CHO) and a caspase-9-specific inhibitor (Ac-LEHD-CHO) also resulted in a significant decrease of apoptosis (Fig. 2B), confirming that both the intrinsic and extrinsic pathways are implicated in the proapoptotic effect of DHA and EPA.

Activation of the extrinsic pathway and cross-talk with the intrinsic pathway

Once we established that the extrinsic pathway is implicated in the apoptotic induction of DHA and EPA, we studied the effect on the crucial regulator of this pathway, FLIP. FLIP inhibits caspase-8 activation, blocking the apoptotic signal transduction through the extrinsic pathway. We showed that *FLIP* expression was strongly repressed as early as 2 hours after n-3 PUFA supplementation, allowing the apoptosis cascade to proceed (Fig. 3).

One of the potential triggers of the intrinsic pathway is the already activated extrinsic pathway. The key element in this cross-talk is the Bid protein. Active caspase-8 cleaves Bid resulting in

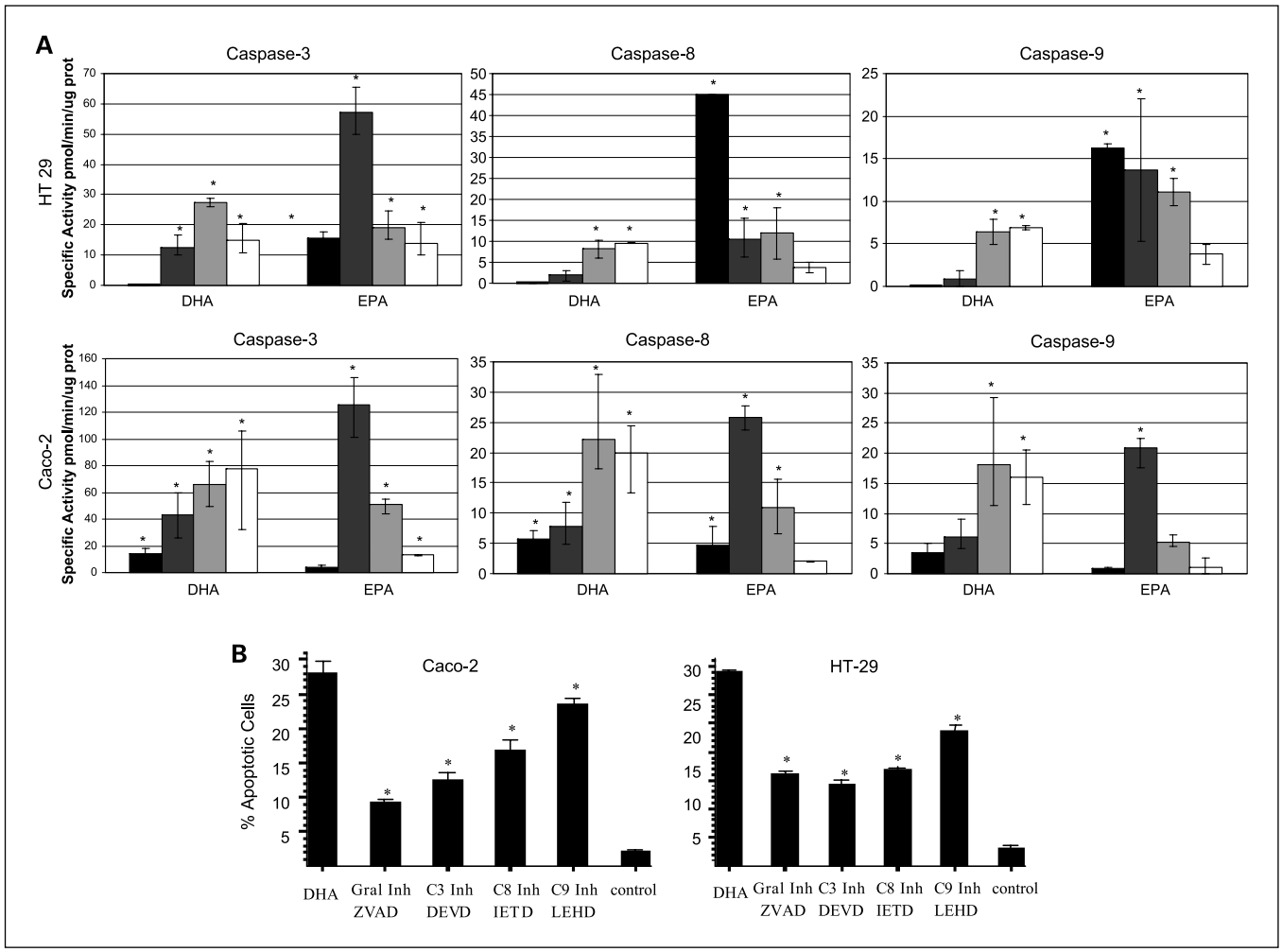

Fig. 2. *A,* graphs representing the specific caspase activity in pmol/min/μg of protein, 2 h (*black bars*), 8 h (*dark gray bars*), 18 h (*light gray bars*), and 24 h (*white bars*) after fatty acid supplementation. Top graphs, HT-29; bottom graphs, Caco-2. Results are corrected for the basal activity values present in control cells. *, statistical significance of $P < 0.05$ with respect to the control. *B,* quantification of apoptotic cells as % over total number of cells 24 h postsupplement with DHA and DHA plus different caspase inhibitors. All caspase inhibitors significantly inhibited apoptosis induced by DHA. *, statistical significance of $P < 0.05$ with respect to the DHA-treated cells.

the active form, tBid. Then tBid can activate the proapoptotic protein Bax, which can trigger the mitochondrial or intrinsic pathway (20). To determine if this cross-talk plays a role in the induction of apoptosis by DHA and EPA, we studied the expression of Bid as well as the Bid-Bax interaction. EPA and DHA supplementation did not induce any important changes in *Bid* gene expression (Fig. 3), but there was a dramatic decrease in full-length Bid protein expression potentially compatible with Bid cleavage and final generation of tBid at 2, 4, and 8 hours postsupplementation (Fig. 4A). Finally, Bid was found to bind to Bax when cells were supplemented with DHA and EPA through immunoprecipitation experiments (Fig. 4B). All together, these experiments strongly suggest cross-talk in the induction of apoptosis by DHA and EPA.

Bax oligomerization and activation of the mitochondrial pathway of apoptosis

Bax homodimerization and possibly Bak homodimerization as well as Bax/Bak heterodimerization constitute the crucial mechanism of mitochondrial outer membrane permeabilization that leads to cytochrome *c* release and the subsequent irreversible apoptosis cascade (21). On the other hand, antiapoptotic Bcl-X_L also plays an important role in controlling this mechanism through its capacity to dimerize with Bax and neutralize it (22, 23). In our study, DHA and EPA-supplementation induced a significant activation of Bax/Bak as shown by the massive coimmunoprecipitation of Bax with Bak and with itself (Fig. 4B) compatible with homodimerization and heterodimerization. There was also a significant increase in binding of Bax

Fig. 3. Graphs representing variation of mRNA RQ at 1, 2, 3, 4, 8, 12, and 18 h after DHA and EPA supplementation; dash, DHA values; dots, EPA values. Results are corrected for an endogenous expression control gene (18S ribosomal) and for the basal expression in control cells (ethanol treated cells). Left graft, Caco-2; right graft, HT-29. *, statistical significance of $P < 0.05$ with respect to DHA or EPA supplementation.

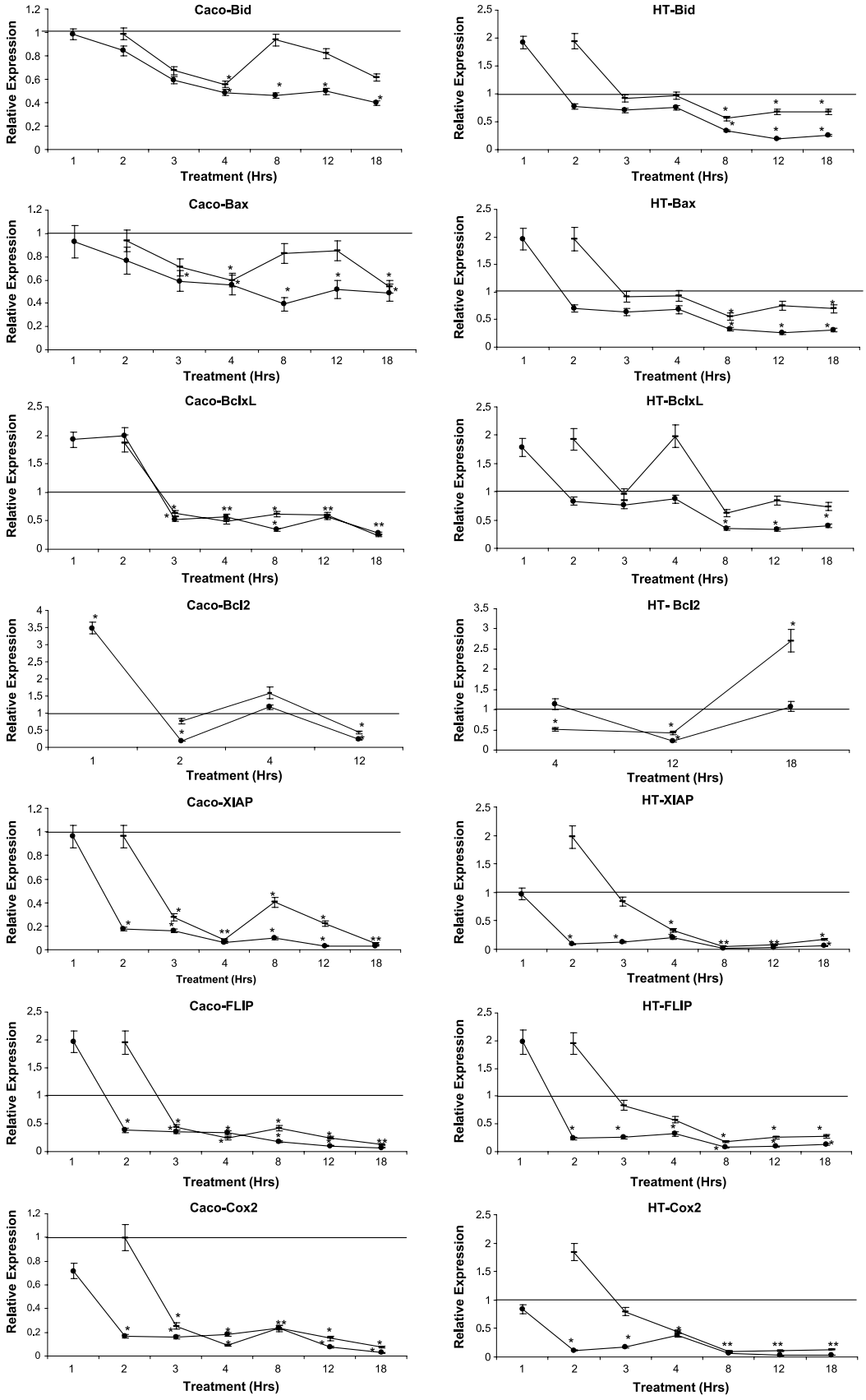

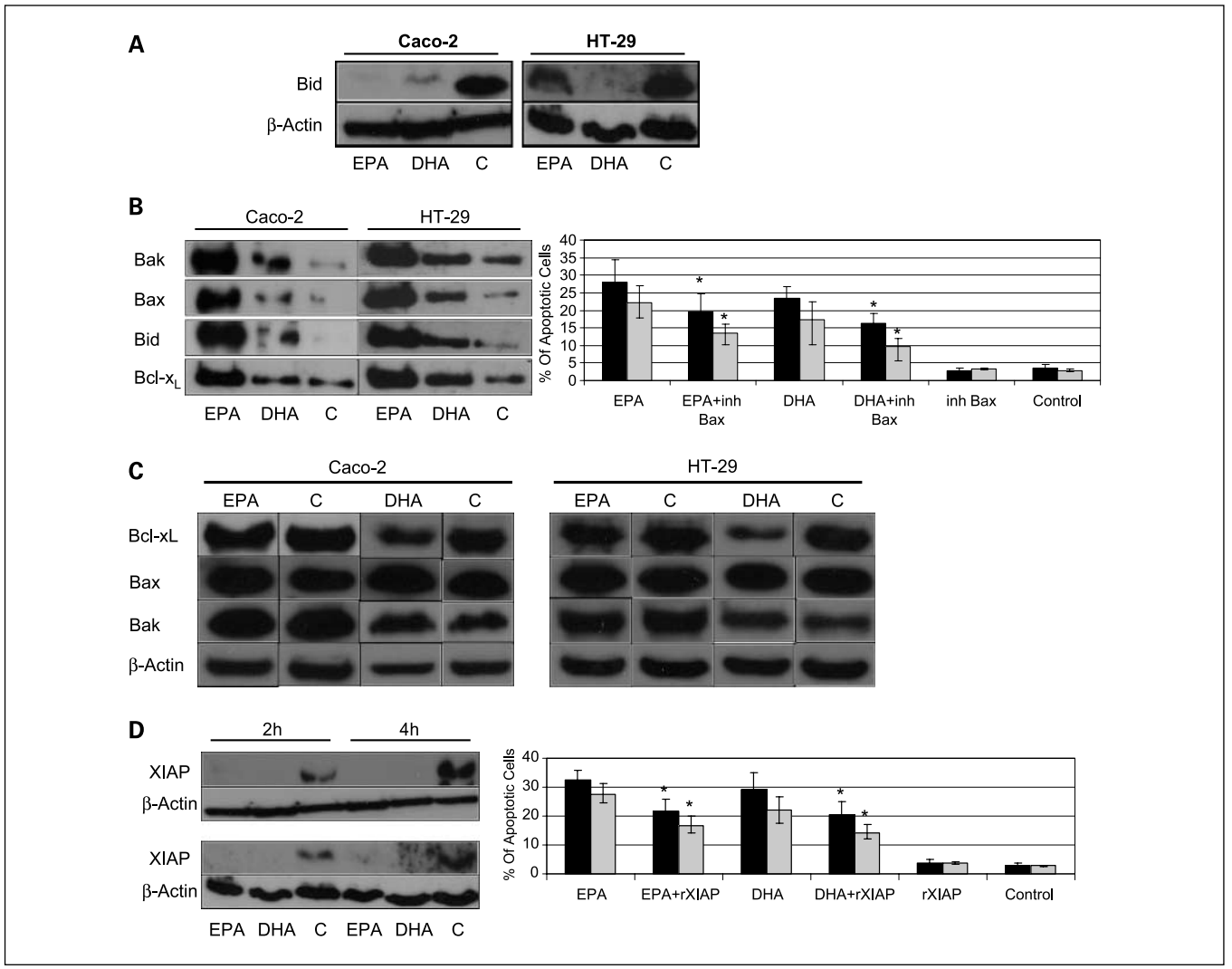

Fig. 4. *A,* immunoblotting from whole cell lysates, hybridized with full-length Bid antibody 2 h after supplementation with DHA and EPA. A decrease in full-length Bid was observed in both cells lines, compatible with cleavage to truncated Bid. *B,* immunoprecipitation of Bax, followed by immunoblotting with Bak, Bax, Bid, and Bcl-X_L antibodies 4 h after supplementation. Graph, the % of apoptotic cells after DHA and EPA alone or in combination with a specific Bax inhibitor. Black bars, HT-29 cells; gray bars, Caco-2 cells. Bax inhibitor partially reverses apoptosis induced by DHA and EPA. *, statistical significance of $P < 0.05$ with respect to DHA or EPA supplementation. *C,* immunoblotting from whole cell lysates, with Bax, Bak, and Bcl-X_L antibodies 4 h after supplementation with DHA and EPA. No changes were seen in the expression of Bax and Bak, but there was a decrease in Bcl-X_L expression. *D,* immunoblotting from whole cell lysate, with XIAP antibody 2 and 4 h after supplementation with DHA and EPA. There was a dramatic decrease in XIAP expression. Graph, the % of apoptotic cells after DHA and EPA alone or in combination with a XIAP recombinant protein. Black bars, HT-29 cells; gray bars, Caco-2 cells. XIAP recombinant protein partially reverses apoptosis induced by DHA and EPA. *, statistical significance of $P < 0.05$ with respect to DHA or EPA supplementation.

with the antiapoptotic Bcl-X_L in the DHA and EPA-supplemented cells in relation to controls (Fig. 4B), possibly in an attempt to offset the massive oligomerization of Bax and Bak that, once started, further amplifies the apoptotic signal through activation of other latent Bax and Bak molecules in an autoactivation mechanism (20). In any case, the decrease in Bcl-X_L suggests that there is less readily available protein to bind to Bax, and the proapoptotic dimerization would out weigh the formation of antiapoptotic complexes.

The implication of Bax in the apoptotic cascade induced by DHA and EPA was further supported after the addition of a specific Bax inhibitor to the supplemented cells, resulting in a significant decrease in apoptosis induction (Fig. 4B, graph). Supplementation of DHA and EPA resulted in minimal changes in *Bax* and *Bcl-X_L* gene expression (Fig. 3). At the protein level, Bax expression was clearly increased 4 hours postsupplementation with DHA and EPA in Caco-2 but not in HT29 cells, whereas Bak expression remained mostly unchanged (Fig. 4C). On the other hand, Bcl-X_L protein levels significantly decreased 4 hours after DHA supplementation, but the effects of EPA were less noticeable most likely due to the earlier changes induced by EPA (Fig. 4C). Some studies have suggested that Cox-2 could induce colonocyte apoptosis through its regulation of the antiapoptotic protein Bcl-2. In fact, forced expression of Cox-2 in intestinal epithelial cells resulted in an induction of Bcl-2 expression and a subsequent inhibition of apoptosis (24). In our experiments, *Cox-2* expression dramatically decreased

after DHA and EPA supplementation in both Caco-2 and HT-29 cells (Fig. 3), but *Bcl-2* expression was only detected with a high number of amplifications, and almost no protein was detected by immunoblotting (data not shown), which implies that *Bcl-2* expression is minimal in the cell lines studied. Therefore, it is unlikely that Bcl-2 plays a significant role in the induction of apoptosis by DHA and EPA in Caco-2 and HT-29 cells.

Mitochondrial membrane permeabilization and induction of the intrinsic pathway cascade

Activation of Bax, and possibly Bak, results in mitochondrial membrane permeabilization (25). Permeabilization allows intermembrane space proteins, including caspase activators (cytochrome *c* and Smac/Diablo), as well as caspase-independent death effectors (apoptosis-inducing factor), to be released into the cytosol. Cytochrome *c* promotes the activation of the initiator caspase-9 in a direct fashion via the assembly of the apoptosome, whereas Smac/Diablo favors the caspase cascade indirectly by antagonizing the activity of endogenous inhibitors of caspases, such as Inhibitor of Apoptosis Proteins (26). To determine if DHA and EPA-induced apoptosis is dependent on mitochondrial membrane permeabilization, we first assessed mitochondrial transmembrane potential with a JC1 stain. Control cells displayed mitochondria stained in red-orange, whereas EPA and DHA-treated cells had a distinct green coloration (Fig. 5A), clearly establishing induction of depolarization by EPA and DHA. As a consequence, there was an increase in cytochrome *c* and Smac/Diablo expression in the cytosolic fraction (Fig. 5B). That fraction had been clearly separated from the mitochondrial fraction as shown by the total absence of cytochrome *c* oxidase subunit IV in the cytosol (Fig. 5C). Finally, the Inhibitor of Apoptosis Protein XIAP was inhibited both at the mRNA and protein levels at 2, 4, and 8 hours postsupplementation (Figs. 3 and 4D). Apoptosis was partially reversed with the addition of recombinant XIAP protein to the DHA and EPA-supplemented cells (Fig. 4D).

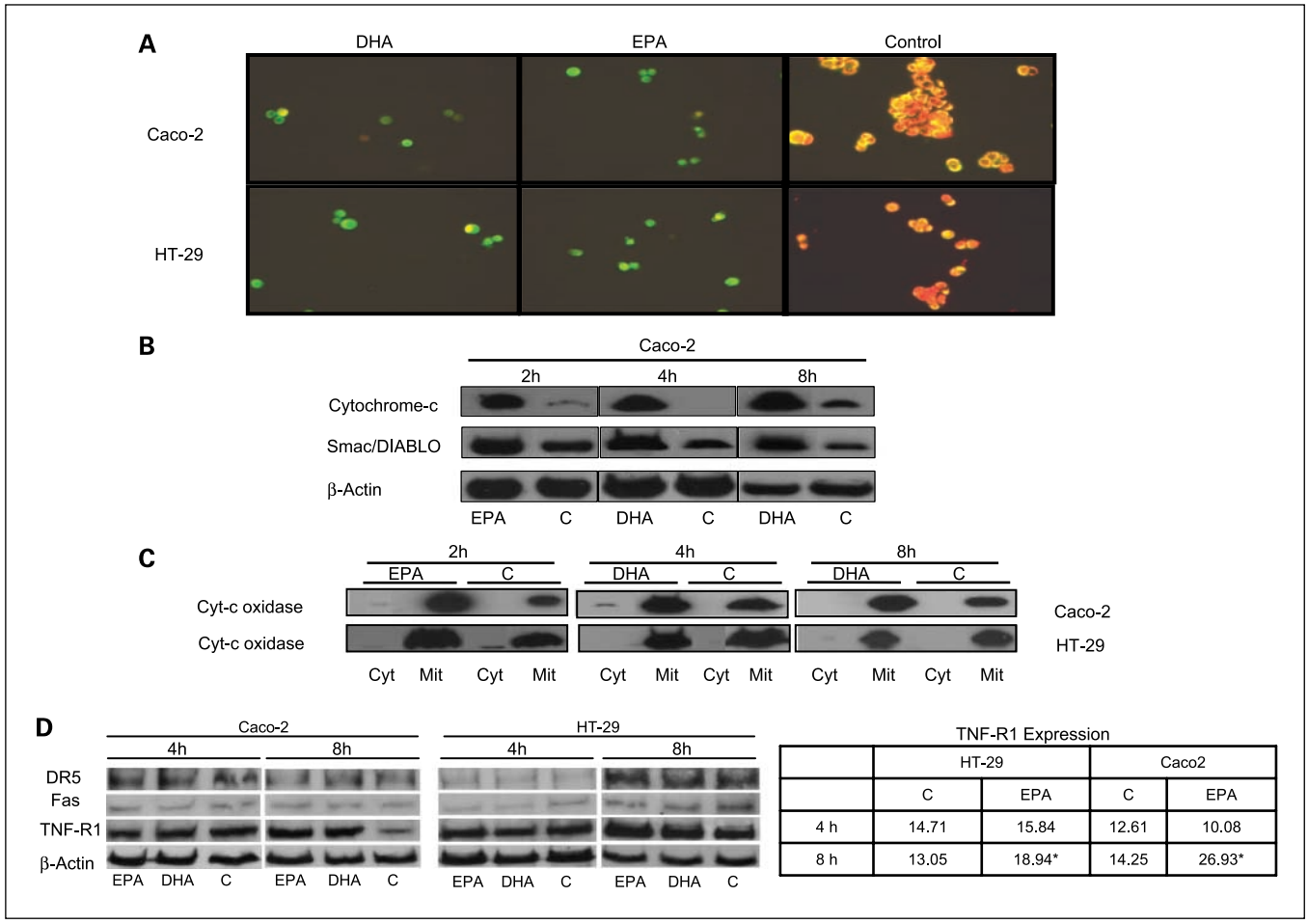

TNF-R1 Expression

	HT-29		Caco2	
	C	EPA	C	EPA
4 h	14.71	15.84	12.61	10.08
8 h	13.05	18.94*	14.25	26.93*

Fig. 5. *A,* fluorescence microscopy of Caco-2 and HT-29 cells stained with JC1, a mitochondrial potential marker stain, 4 h postsupplementation with DHA and EPA. Control cells show an orange coloration, indicating polarization of the mitochondrial membrane, and DHA and EPA-treated cells show a green coloration, as a result of mitochondrial membrane depolarization. *B,* immunoblotting of protein cytosolic fraction with cytochrome *c* and Smac/DIABLO antibodies. The increase of cytochrome *c* and Smac/DIABLO in the cytosolic fraction reflects their translocation to the cytosol. *C,* immunoblotting of cytosolic and mitochondrial fractions with cytochrome *c* oxidase antibody, used as a mitochondrial marker, to prove actual separation of the two fractions. Left, 2 h post-EPA supplementation; middle and right, 4 and 8 h post-DHA supplementation. *D,* immunoblotting with DR5, FAS, and TNF-R1 antibodies, as well as control β-actin 4 and 8 h after DHA and EPA supplementation. There is an increase of expression of TNF-R1, 8 h after fatty acid supplementation in relation to control. The table represents actual fluorescence intensity, as analyzed by FACS scan, of TNF-R1, 4 and 8 h post-EPA supplementation. The results are coincidental with the immunoblots.

Implication of cellular death receptors

To determine the potential implication of cellular death receptors in the induction of apoptosis by DHA and EPA, we studied the expression of FAS, TRAIL-R2 (DR5), and TNF-R1 by Western blot 2, 4, and 8 hours postsupplementation.

Although there were no changes in DR5 and FAS protein expression, TNF-R1 was significantly up-regulated 8 hours after DHA and EPA supplementation in both Caco-2 and HT-29 cells (Fig. 5D). No changes were seen at earlier times, which implies that up-regulation of TNF-R1 is not involved in the

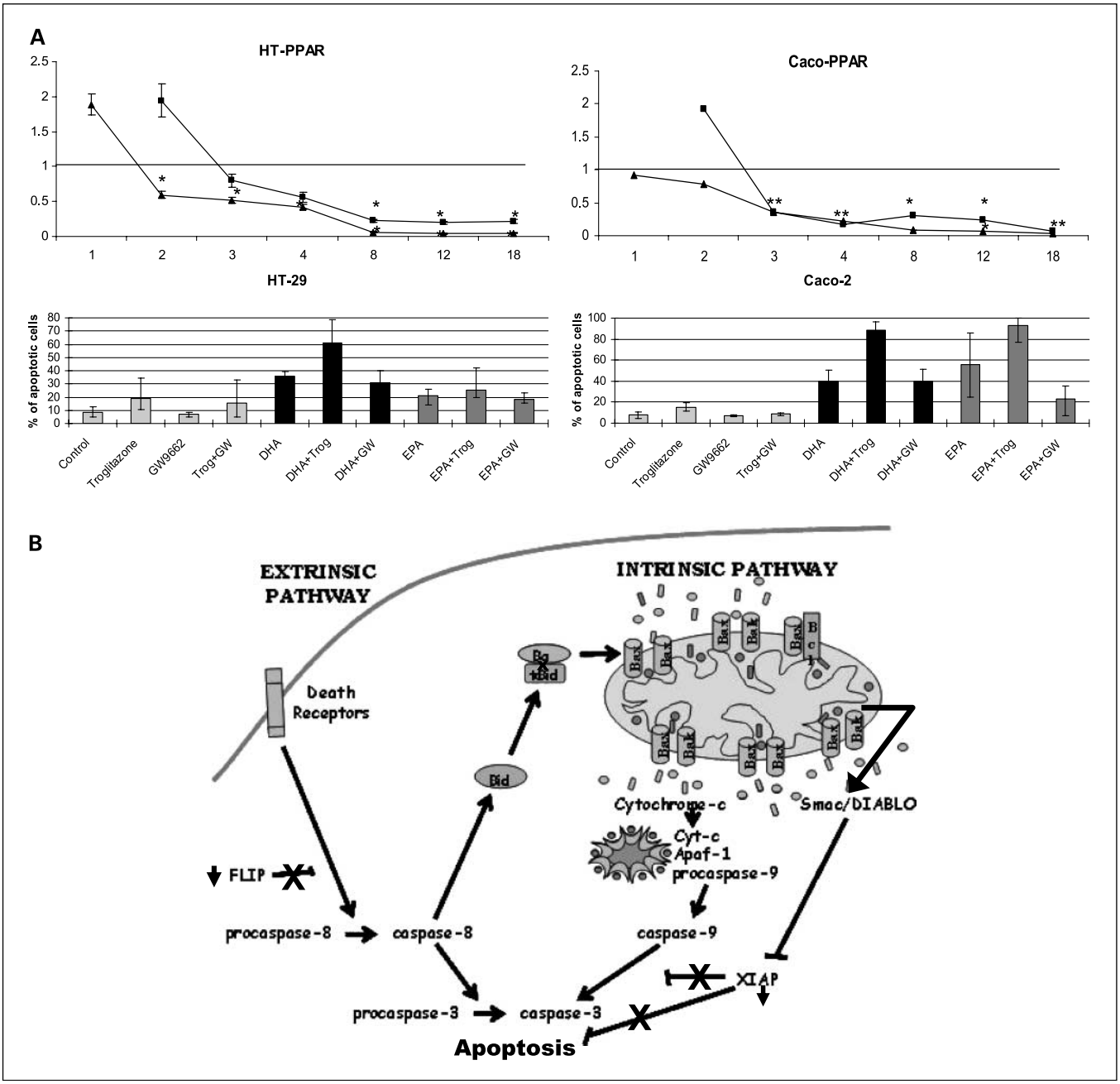

Fig. 6. *A,* top, graphs representing the decrease in PPARγ mRNA RQ 1, 2, 3, 4, 8, 12, and 18 h after DHA and EPA supplementation respect to the control cells. ▪, DHA values; ▲, EPA. Results are corrected for an endogenous expression control gene (18S ribosomal) and for the basal expression in control cells (ethanol-treated cells). Bottom, the quantification of apoptotic cells as % over total number of cells 24 h postsupplementation. Cells are supplemented with troglitzaone (PPAR-γ activator), GW9662 (PPAR-γ antagonist), DHA, EPA, as well as the simultaneous addition of these fatty acids with the PPAR-γ activator and antagonist. *, statistical significance of $P < 0.05$ with respect to DHA and EPA-supplemented cells. *B,* proposed flow graph of the induction of apoptosis by DHA and EPA in colorectal cancers cells. A plausible scenario could be the following: down-regulation of FLIP would allow the activation of caspase-8 and subsequent activation of the extrinsic pathway cascade of apoptosis. Active caspase-8 could also be responsible for the cleavage of Bid that subsequently would bind to Bax, inducing conformational changes and allowing Bax to insert into the mitochondrial membrane where it would bind to Bak and itself. These complexes would form membrane pores, allowing mitochondrial membrane depolarization and release of cytochrome *c* and Smac/Diablo to cytosol, crucial steps in the activation of the intrinsic pathway of apoptosis. In the cytosol, cytochrome *c* would bind to other proteins assembling the apoptosome complex, which would activate caspase-9 and in turn caspase-3. At the same time, Smac/Diablo would block the activity of the Inhibitor of Apoptosis Proteins that, along with its down-regulation, would further favor the activation of the apoptosis cascade.

initial triggering mechanism of apoptosis induction by the n-3 PUFAs. These results were confirmed with flow cytometry analysis (Fig. 5D, *table*).

Lack of PPARγ implication

PPARγ is a member of the Peroxisome proliferator–activated receptor family that is a natural ligand of PUFAs (9). PPARs are ligand-activated transcription factors implicated in lipid metabolism and homeostasis. Recently, it has been shown that they are also involved in cell proliferation and apoptosis. In fact, some PPARγ modulatory drugs seem to reduce FLIP expression, thereby sensitizing tumor cells to the TNF family of death ligands (27). In our experiments, the addition of PPARγ ligand activator troglitazone resulted in a significant increase in apoptosis, and this effect was abrogated with the simultaneous addition of GW9662, an irreversible PPARγ antagonist (Fig. 6A, *table*). To determine the implication of PPARγ in the induction of apoptosis by DHA and EPA, we first assessed its mRNA expression. There was a significant decrease in PPARγ expression starting 4 hours postsupplementation with n-3 PUFAs (Fig. 6A, *graph*). The addition of Troglitazone to DHA and EPA-supplemented cells resulted in a significant increase in apoptosis, whereas GW9662 did not prevent the induction of apoptosis by DHA and EPA (Fig. 6A, *table*). Overall, these experiments suggest that PPARγ is not responsible for the proapoptotic effect of DHA and EPA in these colorectal cancer cells.

Discussion

The elimination of damaged or mutated cells through apoptosis is a crucial anticarcinogenic mechanism. Several studies have shown that the n-3 fatty acids DHA and EPA can induce colonocyte apoptosis and this could be a determinant factor in their antineoplastic effect on colorectal cancer. The goal of the present study was to determine the mechanisms by which DHA and EPA induce apoptosis.

We showed that DHA and EPA are potent apoptosis inducers in colorectal cancer cells with distinct molecular phenotypes, whereas no significant proapoptotic effect was seen in noncancerous colorectal cells. This suggests their potential usefulness as anticarcinogenic agents in a wide group of colorectal cancers. DHA and EPA-induced apoptosis is mediated by caspases. The fact that the inhibition of either caspase-8 or caspase-9 resulted in a partial decrease in apoptosis implicates both the intrinsic and extrinsic pathways (Fig. 6B). The involvement of the intrinsic pathway was further confirmed by the demonstration of different events that are inherent to these processes: the dimerization of Bax and Bak, the depolarization of the mitochondrial membrane, and the subsequent release of cytochrome *c* and Smac/Diablo to the cytosol. The latter allows the apoptosis cascade to proceed through different and complementary mechanisms: cytochrome *c* promotes caspase-9 activation through the assembly of the apoptosome; and Smac/Diablo antagonizes inhibitors of caspases, such as XIAP. Along with a decrease in XIAP protein expression, there was also a striking down-regulation of XIAP mRNA expression. High XIAP expression has been correlated to poor clinical outcome and resistance to chemotherapy and radiotherapy (28). In fact, some studies have shown that inhibition of XIAP gene expression can increase sensitivity to some chemotherapeutic agents (29, 30). Furthermore, blocking XIAP expression has been found to be an important alternative pathway in the treatment of some chemorefractory cancers (31). Therefore, the important down-regulation of XIAP by DHA and EPA could be of critical importance in their antineoplastic effects on colorectal cancer. Nuclear factor-κB could play a determinant role as PUFAs are natural ligands and modulators of nuclear factor-κB, and this has been shown to modulate XIAP (32) and FLIP expression (33). Work is under way to determine NF-κB's role in this setting.

As caspase activity assays and the use of caspase inhibitors showed, the extrinsic apoptosis pathway is also clearly implicated in the induction of apoptosis by DHA and EPA in colorectal cancer cells. This pathway is commonly activated by death receptors. Death receptors are cell surface receptors that transmit apoptotic signals initiated by death ligands (34). The best-described ones are FAS, TNF-R1, and TRAIL-R2 (DR5). The latter has been implicated in anchorage-dependent apoptosis in colorectal cancer cells (35). Activated death receptors induce the assembly of the death-inducing signaling complex, a molecular structure that promotes the dimerization and activation of the initiator caspase-8 and a downstream cascade of caspases that ultimately leads to cell death (26). We saw that TNF-R1 was up-regulated by DHA and EPA, but only at a late stage (8 hours postsupplementation) when the proapoptotic machinery had already been fully activated. Perhaps this was an enhancing phenomenon triggered by the activation of some pro-apoptotic elements, but clearly this was not an early event. Therefore, none of the best-described death receptors seem to be implicated in the induction of the apoptosis process in colorectal cancer cells by DHA and EPA.

FLIP competes with procaspase-8 and procaspase-10 for binding to FADD, thus squelching death receptor signaling. Forced expression of FLIP renders cells resistant to Fas-mediated apoptosis (36). Several tumors, including colorectal cancers, contain inappropriately elevated levels of FLIP, rendering them resistant to apoptosis induction by death domain signaling. Furthermore, FLIP may inhibit both spontaneous death ligand–independent and death receptor–mediated apoptosis in colorectal cancer cells (37), which suggests that targeting FLIP may have important therapeutic potential for the treatment of colorectal cancer. In fact, several important chemotherapeutic agents have been shown to down-regulate FLIP. For example, the induction of apoptosis in T-cell lymphocytes and breast cancer cells by Taxol (paclitaxel), one of the most active cancer chemotherapeutic agents, occurs through down-regulation of FLIP expression (38). The same effect has been documented with celecoxib in human lung cancer cells (39) and with the IκB kinase inhibitor BMS-345541 in mantle cell lymphoma cells (40). The immediate and dramatic down-regulation of FLIP after DHA and EPA supplementation seems to be a crucial mechanism in the induction of apoptosis by these fatty acids. This mechanism is consistent with the above-mentioned chemotherapeutic agents, and it seems to be independent of PPARγ. Although a PPARγ activating ligand also induced apoptosis in these cells, this effect was unrelated to the proapoptotic effect of DHA and EPA. Furthermore, apoptosis was induced in cells not expressing Cox-2 and/or Bcl-2, which questions a significant role of Cox-2, through its down-regulation of Bcl-2, in the induction of apoptosis by DHA and EPA.

In summary, DHA and EPA induce apoptosis in different types of colorectal cancer cells but not in nonmalignant colonocytes. This effect seems to be related with a dramatic inhibition of two critical elements controlling the apoptosis cascade, FLIP, and XIAP, and both the intrinsic and extrinsic pathways are activated. None of the death receptors commonly implicated in apoptotic signaling seem to be activated by these fatty acids. These findings raise new possibilities regarding the potential use of DHA and EPA along with other anticarcinogenic products for colorectal cancer prevention and/or therapy.

Disclosure of Potential Conflicts of Interest

No potential conflicts of interest were disclosed.

References

1. Greenlee RT, Murray T, Bolden S, Wingo PA. Cancer statistics, 2000. CA Cancer J Clin 2000; 50:7–33.
2. Parkin DM. International variation. Oncogene 2004;23:6329–40.
3. Hall MN, Chavarro JE, Lee IM, Willett WC, Ma J. A 22-year prospective study of fish, n-3 fatty acid intake, and colorectal cancer risk in men. Cancer Epidemiol Biomarkers Prev 2008;17:1136–43.
4. Fernandez E, Chatenoud L, La Vecchia C, Negri E, Franceschi S. Fish consumption and cancer risk. Am J Clin Nutr 1999;70:85–90.
5. Willett WC, Stampfer MJ, Colditz G, Colditz GA, Rosner BA, Speizer FE. Relation of meat, fat, and fiber intake to the risk of colon cancer in a prospective study among women. N Engl J Med 1990;323: 1664–72.
6. Kato I, Akhmedkhanov A, Koenig K, Toniolo PG, Shore RE, Riboli E. Prospective study of diet and female colorectal cancer: the New York University Women's Health Study. Nutr Cancer 1997;28: 276–81.
7. Rose DP, Connolly JM. Omega-3 fatty acids as cancer chemopreventive agents. Pharmacol Ther 1999;83:217–44.
8. Siddiqui RA, Shaikh SR, Sech LA, Yount HR, Stillwell W, Zaloga GP. Omega 3-fatty acids: health benefits and cellular mechanisms of action. Mini Rev Med Chem 2004;4:859–71.
9. Larsson SC, Kumlin M, Ingelman-Sundberg M, Wolk A. Dietary long-chain n-3 fatty acids for the prevention of cancer: a review of potential mechanisms. Am J Clin Nutr 2004;79:935–45.
10. Hall MN, Campos H, Li H, et al. Blood levels of long-chain polyunsaturated fatty acids, aspirin, and the risk of colorectal cancer. Cancer Epidemiol Biomarkers Prev 2007;16:314–21.
11. Christiansen EN, Lund JS, Rortveit T, Rustan AC. Effect of dietary n-3 and n-6 fatty acids on fatty acid desaturation in rat liver. Biochim Biophys Acta 1991;1082:57–62.
12. Grosch S, Maier TJ, Schiffmann S, Geisslinger G. Cyclooxygenase-2 (COX-2)-independent anticarcinogenic effects of selective COX-2 inhibitors. J Natl Cancer Inst 2006;98:736–47.
13. Courtney ED, Matthews S, Finlayson C, et al. Eicosapentaenoic acid (EPA) reduces crypt cell proliferation and increases apoptosis in normal colonic mucosa in subjects with a history of colorectal adenomas. Int J Colorectal Dis 2007;22:765–76, Epub 2007 Jan 10.
14. Calviello G, Palozza P, Maggiano N, et al. Cell proliferation, differentiation, and apoptosis are modified by n-3 polyunsaturated fatty acids in normal colonic mucosa. Lipids 1999;34:599–604.
15. Chang WL, Chapkin RS, Lupton JR. Fish oil blocks azoxymethane-induced rat colon tumorigenesis by increasing cell differentiation and apoptosis rather than decreasing cell proliferation. J Nutr 1998;128:491–7.
16. Latham P, Lund EK, Johnson IT. Dietary n-3 PUFA increases the apoptotic response to 1,2-dimethylhydrazine, reduces mitosis and suppresses the induction of carcinogenesis in the rat colon. Carcinogenesis 1999;20:645–50.
17. Llor X, Pons E, Roca A, et al. The effects of fish oil, olive oil, oleic acid and linoleic acid on colorectal neoplastic processes. Clin Nutr 2003;22:71–9.
18. Narayanan BA, Narayanan NK, Reddy BS. Docosahexaenoic acid regulated genes and transcription factors inducing apoptosis in human colon cancer cells. Int J Oncol 2001;19:1255–62.
19. Pfaffl MW. A new mathematical model for relative quantification in real-time RT-PCR. Nucleic Acids Res 2001;29:e45.
20. Danial NN. BCL-2 family proteins: critical checkpoints of apoptotic cell death. Clin Cancer Res 2007;13:7254–63.
21. Chandra D, Choy G, Daniel PT, Tang DG. Bax-dependent regulation of Bak by voltage-dependent anion channel 2. J Biol Chem 2005;280:19051–61, Epub 2005 Mar 9.
22. Willis SN, Chen L, Dewson G, et al. Proapoptotic Bak is sequestered by Mcl-1 and Bcl-xL, but not Bcl-2, until displaced by BH3-only proteins. Genes Dev 2005;19:1294–305, Epub 2005 May 18.
23. Zhang XJ, Yan J, Cuttle L, Endre Z, Gobe G. Escape from apoptosis after prolonged serum deprivation is associated with the regulation of the mitochondrial death pathway by Bcl-x(l). Biochem Biophys Res Commun 2000;277:487–93.
24. Tsujii M, DuBois RN. Alterations in cellular adhesion and apoptosis in epithelial cells overexpressing prostaglandin endoperoxide synthase 2. Cell 1995;83:493–501.
25. Rasola A, Bernardi P. The mitochondrial permeability transition pore and its involvement in cell death and in disease pathogenesis. Apoptosis 2007;12:815–33.
26. Galluzzi L, Zamzami N, de La Motte Rouge T, Lemaire C, Brenner C, Kroemer G. Methods for the assessment of mitochondrial membrane permeabilization in apoptosis. Apoptosis 2007;12:803–13.
27. Kim Y, Suh N, Sporn M, Reed JC. An inducible pathway for degradation of FLIP protein sensitizes tumor cells to TRAIL-induced apoptosis. J Biol Chem 2002;277:22320–9, Epub 2002 Apr 8.
28. Danson S, Dean E, Dive C, Ranson M. IAPs as a target for anticancer therapy. Curr Cancer Drug Targets 2007;7:785–94.
29. Lacasse EC, Kandimalla ER, Winocour P, et al. Application of XIAP antisense to cancer and other proliferative disorders: development of AEG35156/GEM640. Ann N Y Acad Sci 2005;1058:215–34.
30. Shrikhande SV, Kleeff J, Kayed H, et al. Silencing of X-linked inhibitor of apoptosis (XIAP) decreases gemcitabine resistance of pancreatic cancer cells. Anticancer Res 2006;26:3265–73.
31. Cillessen SA, Hess CJ, Hooijberg E, et al. Inhibition of the intrinsic apoptosis pathway downstream of caspase-9 activation causes chemotherapy resistance in diffuse large B-cell lymphoma. Clin Cancer Res 2007;13:7012–21.
32. Gordon GJ, Mani M, Mukhopadhyay L, et al. Inhibitor of apoptosis proteins are regulated by tumour necrosis factor-α in malignant pleural mesothelioma. J Pathol 2007;211:439–46.
33. Micheau O, Lens S, Gaide O, Alevizopoulos K, Tschopp J. NF-κB signals induce the expression of c-FLIP. Mol Cell Biol 2001;21:5299–305.
34. Ashkenazi A, Dixit VM. Death receptors: signaling and modulation. Science 1998;281:1305–8.
35. Laguinge LM, Samara RN, Wang W, et al. DR5 receptor mediates anoikis in human colorectal carcinoma cell lines. Cancer Res 2008;68:909–17.
36. Panka DJ, Mano T, Suhara T, Walsh K, Mier JW. Phosphatidylinositol 3-kinase/Akt activity regulates c-FLIP expression in tumor cells. J Biol Chem 2001; 276:6893–6, Epub 2001 Jan 5.
37. Wilson TR, McLaughlin KM, McEwan M, et al. c-FLIP: a key regulator of colorectal cancer cell death. Cancer Res 2007;67:5754–62.
38. Day TW, Najafi F, Wu CH, Safa AR. Cellular FLICE-like inhibitory protein (c-FLIP): a novel target for Taxol-induced apoptosis. Biochem Pharmacol 2006;71:1551–61. Epub 2006 Mar 31.
39. Liu X, Yue P, Schonthal AH, Khuri FR, Sun SY. Cellular FLICE-inhibitory protein down-regulation contributes to celecoxib-induced apoptosis in human lung cancer cells. Cancer Res 2006;66: 11115–9.
40. Roue G, Perez-Galan P, Lopez-Guerra M, Villamor N, Campo E, Colomer D. Selective inhibition of IκB kinase sensitizes mantle cell lymphoma B cells to TRAIL by decreasing cellular FLIP level. J Immunol 2007;178:1923–30.